Int J Clin Exp Med 2018;11(7):6740-6748
www.ijcem.com /ISSN:1940-5901/IJCEM0066729

Original Article

Pax2 expression correlates with EMT markers in an experimental model of obstructive nephropathy

Li Li[1], Hai-Sheng Xu[1], Yu-Bin Wu[2], Xiao-Ming Kang[1], Jun Yang[3], Xian-He Wang[1], Qing-Yun Meng[1], Chang-Shan Wang[4]

[1]Department of Pediatrics, First Affiliated Hospital of Jiamusi University, Jiamusi 154002, China; [2]Department of Pediatric Nephrology, Shengjing Hospital, China Medical University, Shenyang 110004, China; [3]Department of Cardiovascular Medicine, First Affiliated Hospital of Jiamusi University, Jiamusi 154002, China; [4]College of Basic Medicine, Jiamusi University, Jiamusi 154007, Heilongjiang, China

Received October 7, 2017; Accepted May 16, 2018; Epub July 15, 2018; Published July 30, 2018

Abstract: Introduction: This study investigated the role of PAX2 reexpression during tubular epithelial-mesenchymal transition (EMT) in a unilateral ureteral obstruction (UUO) rat model. Methods: Wistar rats were randomly designated into the sham group and UUO model group, and their kidneys were removed for histological evaluation of renal damage. The mRNA and protein levels of PAX2, E-cadherin and α-SMA were then quantified. In addition, the expression of PAX2, E-cadherin and α-SMA protein was detected by immunohistochemical analysis. Results: The kidneys of rats from the UUO group revealed significantly higher histological injury scores (6.17 ± 0.86) and larger areas of renal interstitial collagen deposition (33.75 ± 2.37%) compared with the sham group at 14 days (0.15 ± 0.10 and 1.78 ± 0.37%, respectively, both $P < 0.05$). UUO led to a rapid increase in PAX2 mRNA and protein expression, accompanied with a down-regulation of the epithelial marker E-cadherin and an up-regulation of the mesenchymal marker α-SMA ($P < 0.05$). Immunohistochemical double staining of these samples revealed enlarged areas that stained positively for both PAX2 and α-SMA, but showed decreased E-cadherin expression. The protein levels of PAX2 in renal tubules was positively associated with α-SMA expression ($r = 0.977$, $P < 0.05$) and negatively associated with E-cadherin ($r = -0.984$, $P < 0.05$). Conclusion: PAX2 is re-expressed in the renal tubular epithelial cells following obstructive nephropathy, and may participate in EMT during renal interstitial fibrosis.

Keywords: Unilateral ureteral obstruction, epithelial-mesenchymal transition, renal interstitial fibrosis, paired box 2 gene

Introduction

Renal interstitial fibrosis (RIF) is the final manifestation of chronic kidney disease (CKD), which leads to renal failure [1, 2]. RIF is characterized by inflammatory cell infiltration, the accumulation of extracellular matrix (ECM) compounds, as well as fibroblast activation and proliferation [3, 4]. Renal interstitial cells are a heterogeneous population that contains fibroblasts, dendritic cells, and lymphocytes, in addition to other cell types. Long-term activation of renal interstitial fibroblasts results in excessive ECM accumulation, ultimately causing chronic renal fibrosis, perturbed parenchymal tissue structure, and impaired organ function.

Tubular epithelial-mesenchymal transition (EMT) is a known initiator of RIF [5-7]. EMT is a process in which renal tubular cells lose their epithelial phenotype, involving downregulation of E-cadherin, and instead acquire phenotypic characteristics of mesenchymal cells, such as expression of α-smooth muscle actin (α-SMA) [6, 8]. During EMT, tubular epithelial cells lose their contact with neighboring cells and underlying basement membrane, migrate and invade the interstitium where they ultimately turned into activated fibroblasts [9].

Although EMT contributes to renal fibrosis and causes a reduction in renal parenchyma, the cellular mechanisms that regulate tubular EMT have yet to be fully elucidated.

In the kidney organogenesis, a series of morphogenetic and differentiation events start, so that the mesenchymal blastema is induced to undergo mesenchymal-to-epithelial transi-

Table 1. Real-time PCR primers

Genes	Primers	Length
PAX2-F	5'-CGGTGAGAAGAGGAAACGAG-3'	246 bp
PAX2-R	5'-GCTTGGAAGACATCG GGATA-3'	
E-cadherin-F	5'-TGCTCCTACTGTTTCTACG-3'	111 bp
E-cadherin-R	5'-CTTCTCCACCTCCCTCTT-3'	
α-SMA-F	5'-AGCCAGTCGCCATCAGGAAC-3'	90 bp
α-SMA-R	5'-CCGGAGCCATTGTCACACAC-3'	
GAPDH-F	5'-GGCACAGTCAAGGCTGAGAATG-3'	143 bp
GAPDH-R	5'-ATGGTGGTGAAGACGCCAGTA-3'	

tion (MET) conversion or transition. This earliest MET follows a structurally well-defined morphogenetic pathway to generate most of the nephron. The transcription factor paired box 2 (PAX2), plays a crucial role in inducing MET in renal tubular cells during embryonic kidney development [10]. Normal PAX2 expression is required for regular kidney development. Nevertheless, overexpression of PAX2 has been associated with RIF in renal tissue, thus suggesting that PAX2 contributes to RIF onset and progression [11].

In this study, we established a unilateral ureteral obstruction (UUO) rat model to simulate the pathophysiological features of RIF. We tested whether re-expression of PAX2 plays a role in RIF by promoting EMT in a UUO rat model. Furthermore, we investigate whether the correlation between the levels of PAX2 expression with those of both α-SMA and E-cadherin has any physiological relevance.

Methods and materials

Experimental animals

A total of 64 male Wistar rats (specific pathogen-free (SPF) level, weight range between 120-150 g, 4-6 weeks old) were provided by the Animal Experimental Center of Jiamusi University. The rats were randomly divided into either the sham group (n = 32) or the UUO group (n = 32) using a random numbers table. This study was carried out in strict accordance with the National Institutes of Health (NIH) Guide for the Care and Use of Laboratory Animals. The protocol was approved by the Committee on the Ethics of Animal Experiments of the Jiamusi University (Permit Number: JMSU-186).

Surgical procedures and sample preparation

All surgery was performed under sodium pentobarbital anesthesia, and all efforts were made to minimize suffering. After anaesthetized, the left ureter was identified through a small suprapubic incision and was ligated with 4-0 suture at two points, and then cut between the two points in order to prevent retrograde infection. Operations performed on the sham group excluded the ureteral ligation and cutting steps. At day 3, 5, 7 and 14 following operation, eight rats were sacrificed per group with an overdose of pentobarbital sodium, and their left kidneys were subsequently harvested.

Histological analysis

Sections of left kidney tissue were stained with haematoxylin and eosin (H&E) for subsequent imaging using a light microscope (Olympus, Tokyo, Japan). Images were used to evaluate the severity of renal interstitial injury according to the following three parameters: tubule proteinaceous casts and dilation, interstitial inflammation, and interstitial fibrosis. Each parameter was assigned a score from 0 to 3 according to severity (0 = none, 1 = mild, 2 = moderate, 3 = severe), and these scores were added together to yield an overall tubulointerstitial score between 0 and 9. To determine the degree of collagen accumulation, kidney sections were stained with Masson's trichrome (Zhongshan Biochemical, Beijing, China) and quantitatively measured using NIS-Elements BR 2.10 software (Nikon, Tokyo, Japan). Ten independent images (400× magnification) were randomly selected from each sample. The ratio of the interstitial collagen deposit area (colored in blue) to the total renal interstitial area was determined, and the mean values of these estimates were then used in subsequent analyses.

Immunohistochemical analysis

The following primary antibodies were utilized throughout these studies: rabbit anti-rats PAX2 monoclonal antibody (dilution 1:100, Zymed Laboratories, San Francisco, CA, USA); mouse anti-rat E-cadherin (dilution 1:100, Santa Cruz, CA, USA) and α-SMA monoclonal antibody (dilu-

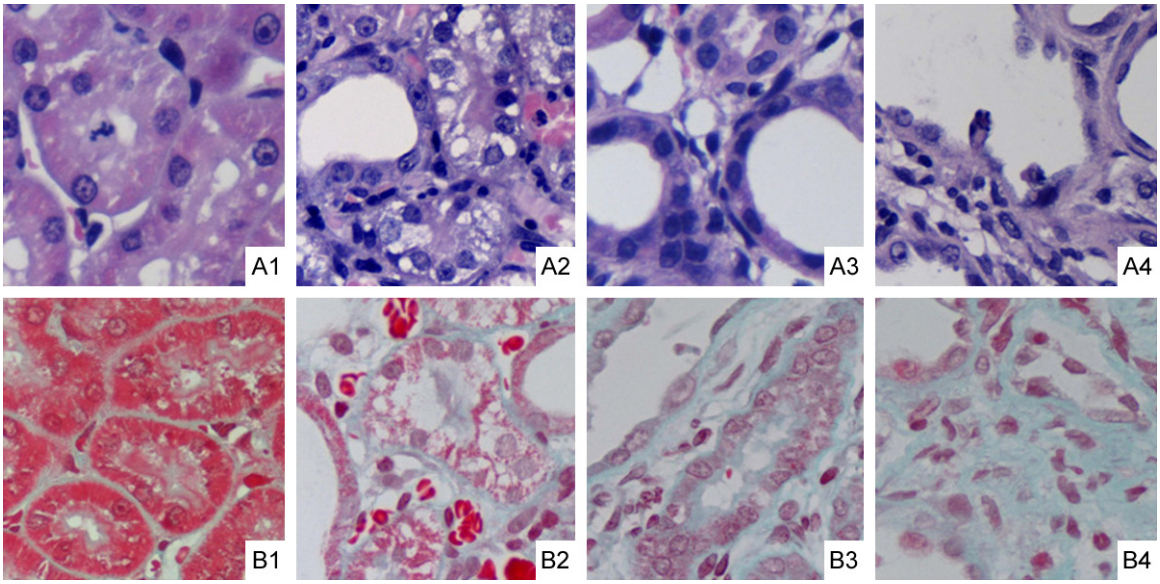

Figure 1. Histological analysis of kidney tissue by haematoxylin and eosin (A1-A4) and Masson's trichrome staining (B1-B4). Magnification, 400×. A1. Normal morphology of tubule structures in the sham group; A2. Day 3 following UUO, tubulointerstitial inflammatory cell infiltration; A3. Day 7 following UUO, tubular dilation and interstitial edema; A4. Day 14 following UUO, severe damage of tubule structure, tubular atrophy, collapse of tubular lumen, massive necrosis of epithelial cells, infiltration of macrophages and lymphocytes, and fibroblast proliferation. B1. Renal section from sham-operated rats; B2. Day 3 following UUO, a small amount of interstitial collagen accumulation in kidney tissue; B3. Day 7 following UUO, increased interstitial collagen accumulation; B4. Day 14 following UUO, significant increase in extracellular matrix components.

tion 1:100, Santa Cruz, CA, USA). Immunohistochemical staining was performed according to the manufacturer's instructions (Zhongshan Golden Bridge Biotechnology, Beijing, China). Briefly, following antigen retrieval, the sections were incubated with PAX2 and either E-cadherin or α-SMA primary antibodies at 4°C overnight. Then the sections were incubated with both biotinylated goat anti-rabbit secondary antibody and alkaline phosphatase (AP)-conjugated goat anti-mouse secondary antibody (1:1 volume) for 30 min. The reaction was then visualized using 3, 3'-Diaminobenzidine (DAB) and AP red. The sections were rinsed with water and counterstained with Mayer's hematoxylin.

Western blotting

Samples of renal cortex isolated from rats (100 mg per sample) were lysed, and total protein was quantified using the bicinchonic acid (BCA) method. Protein samples (50 g) were loaded onto a polyacrylamide gel and subjected to sodium dodecyl sulfate polyacrylamide gel electrophoresis (SDS-PAGE). Proteins were then electroblotted onto a polyvinylidene difluoride (PVDF) membrane. The membrane was blocked with 5% fat-free milk at 4°C overnight, followed by incubation with PAX2, α-SMA, E-cadherin and β-actin (control) primary antibodies (all diluted at 1:1000) at 37°C for 2 h. Membranes were then washed three times and incubated at room temperature for 1 h with horseradish peroxidase-conjugated secondary antibodies (1:500 dilution, Santa Cruz, CA, USA). The density of the corresponding bands was measured using image analysis software (Quantity One-4.4.0, Bio-Rad Laboratories, Hercules, CA, USA) and corrected according to the value of the β-actin control.

Real-time polymerase chain reaction (PCR)

Total RNA (500 ng) was extracted, and was reverse-transcribed into complementary DNA (cDNA) using the PrimeScriptTM RT Reagent KIT (Takara, Otsu, Shiga, Japan). The primer sequences that were used for RT-PCR analyses are shown in **Table 1**. Real-Time PCR was performed using the ABI 7500 real-time PCR system (Applied Biosystems, Foster City, CA, USA). Thermal cycling conditions included: 40 cycles of 95°C for 10 sec, 95°C for 5 sec and 60°C for 34 sec. Melt Curve: 95°C for 15 sec,

Table 2. Renal tubular injury score in each group (0-9, mean ± SEM, n = 8)

	3 d	5 d	7 d	14 d
Sham	0.12 ± 0.03	0.13 ± 0.05	0.11 ± 0.02	0.15 ± 0.10
UUO	2.53 ± 0.26*	3.75 ± 0.65**	4.61 ± 0.73**	6.17 ± 0.86**

*$P < 0.05$, compared to the sham group; **$P < 0.05$, intra-group comparison in UUO group.

Table 3. Relative area of renal interstitium in each group (%, mean ± SEM, n = 8)

	3 d	5 d	7 d	14 d
Sham	1.70 ± 0.21	1.51 ± 0.33	1.55 ± 0.72	1.78 ± 0.37
UUO	7.57 ± 1.01*	15.28 ± 1.76**	23.67 ± 2.11**	33.75 ± 2.37**

*$P < 0.05$, compared to the sham group; **$P < 0.05$, intra-group comparison in UUO group.

60°C for 1 min, and 95°C for 15 sec. A standard curve was generated by using serial dilutions of an established template. The relative mRNA concentration in each sample was calculated using the $2^{-\Delta\Delta CT}$ method.

Statistical analysis

Statistical analyses were performed using the SPSS software package (version 17.0; SPSS Inc, USA). Data were analyzed using t tests and one-way analyses of variance (ANOVA) to evaluate inter-group and intra-group differences, respectively. Correlations between data were analyzed using the Pearson test. $P < 0.05$ was used as the threshold for determining statistical significance.

Results

Histologically abnormalities in UUO-treated kidneys

The kidneys of rats in the control group showed a normal shape with a notably smooth surface. This was in stark contrast to the appearance of kidneys from the UUO-treated rats, which were dilated and showed dramatic thinning of the renal parenchyma and hydronephrosis.

In the H&E-stained sections, the sham group exhibited normal tubules with proper morphology and organization (**Figure 1A**). However, at day 3 following the operation, the UUO group showed signatures of tubular dilation in addition to tubulointerstitial lymphocyte and monocyte infiltration. At day 14, UUO group tubule structures were severely damaged, showing signs of tubular atrophy, collapse of tubular lumen, massive necrosis of epithelial cells, infiltration of macrophages and lymphocytes, fibroblast proliferation and excessive collagen deposit. The UUO group had a significantly higher histological injury score compared with the control sham group ($P < 0.05$ at each time point after UUO, **Table 2**).

In the sham group, Masson trichrome staining was primarily localized to the basement membrane, mesangial areas and surrounding capillaries, but rarely visible in the interstitium surrounding the tubules (**Figure 1B**). We found that interstitial collagen accumulation in the rat kidney tissue significantly increased following UUO, which persisted with prolonged obstruction. UUO also caused a dramatic widening of the renal interstitium as well as an increase in stromal cell number and ECM components. The UUO group also had a significantly larger area of renal interstitial collagen deposition when compared with the sham group ($P < 0.05$ at each time point after UUO, **Table 3**).

mRNA levels of PAX2, α-SMA and E-cadherin

As shown in **Figure 2**, PAX2 mRNA expression was up-regulated at day 3 following UUO when compared with the sham group ($P < 0.05$). Notably, this increase in mRNA expression became more pronounced with extended obstruction time ($P < 0.05$, at each time point). Furthermore, a similar increase in α-SMA mRNA expression was also detected. Conversely, whereas E-cadherin was highly expressed in the renal cortex of rats in the sham group, its expression was remarkably downregulated following UUO treatment ($P < 0.05$ at all time points).

Protein levels of PAX2, α-SMA and E-cadherin

Upon ligation of the left ureter at day 3, PAX2 protein levels rose rapidly in the affected kidney. By 14 days following UUO, renal PAX2 expression was significantly elevated compar-

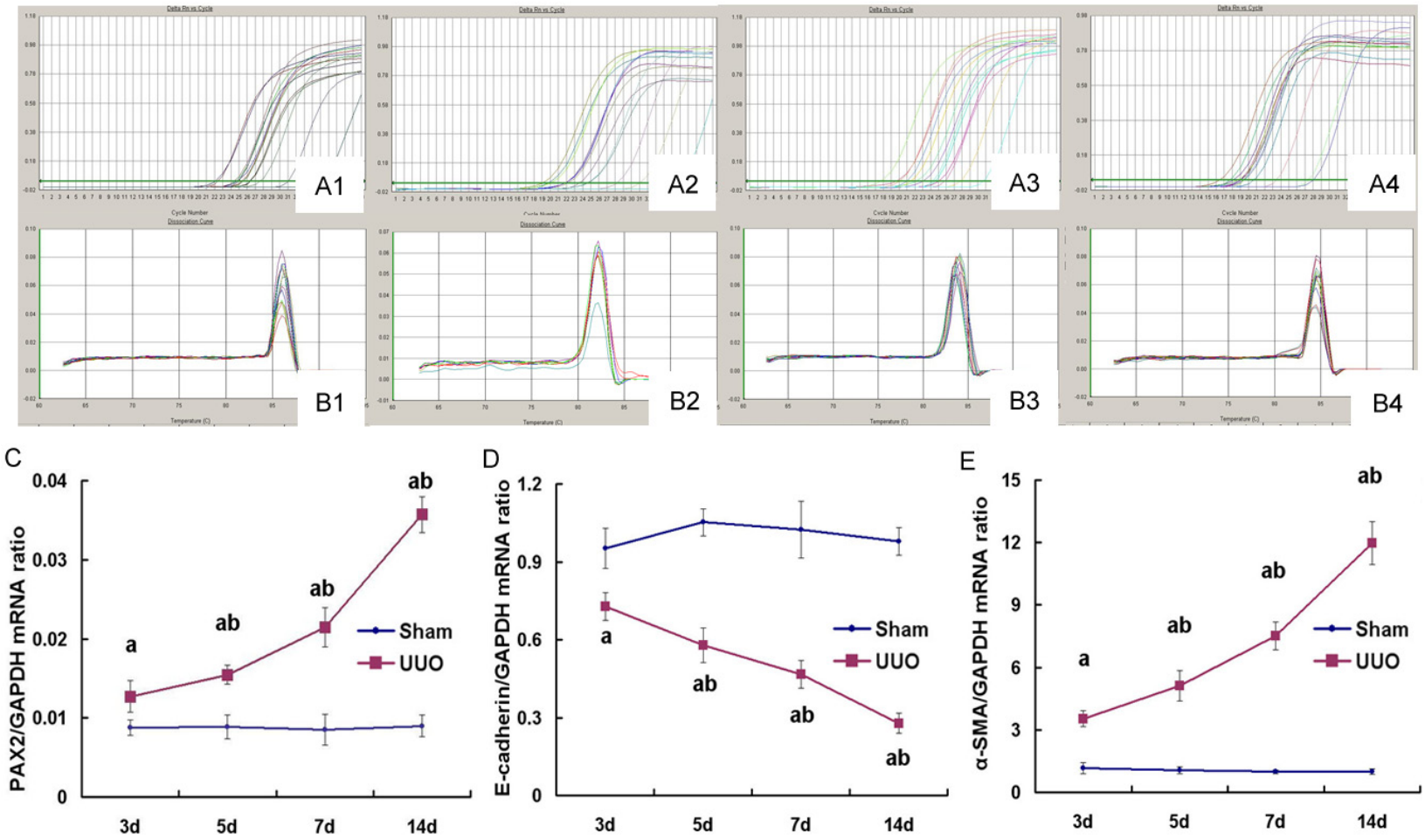

Figure 2. The mRNA expression of PAX2, E-cadherin and α-SMA detected by real time-PCR. Amplification curves of PAX2 (A1), E-cadherin (A2), α-SMA (A3) and GAPDH (A4). Melting curves of PAX2 (B1, 87°C), E-cadherin (B2, 83.5°C), α-SMA (B3, 83.5°C) and GAPDH (B4, 84°C). Quantification of the mRNA levels of PAX2 (C), E-cadherin (D) and α-SMA (E), and corrected by reference to the value of GAPDH. [a]$P < 0.05$ compared to the sham group; [b]$P < 0.05$, intra-group comparison (vs. all other time points) in the UUO group.

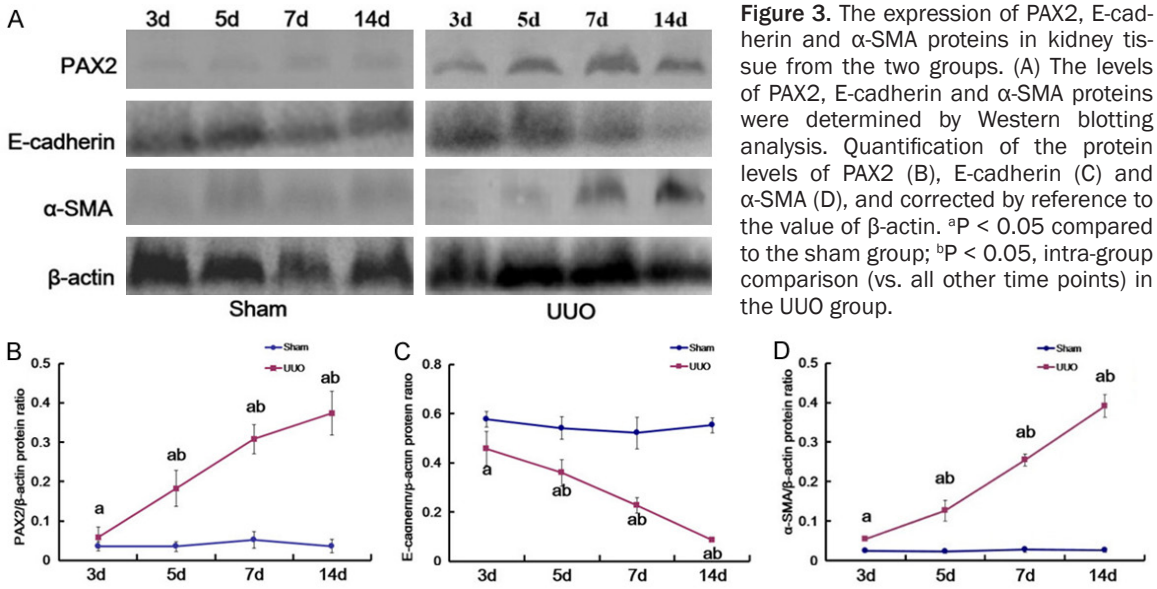

Figure 3. The expression of PAX2, E-cadherin and α-SMA proteins in kidney tissue from the two groups. (A) The levels of PAX2, E-cadherin and α-SMA proteins were determined by Western blotting analysis. Quantification of the protein levels of PAX2 (B), E-cadherin (C) and α-SMA (D), and corrected by reference to the value of β-actin. [a]P < 0.05 compared to the sham group; [b]P < 0.05, intra-group comparison (vs. all other time points) in the UUO group.

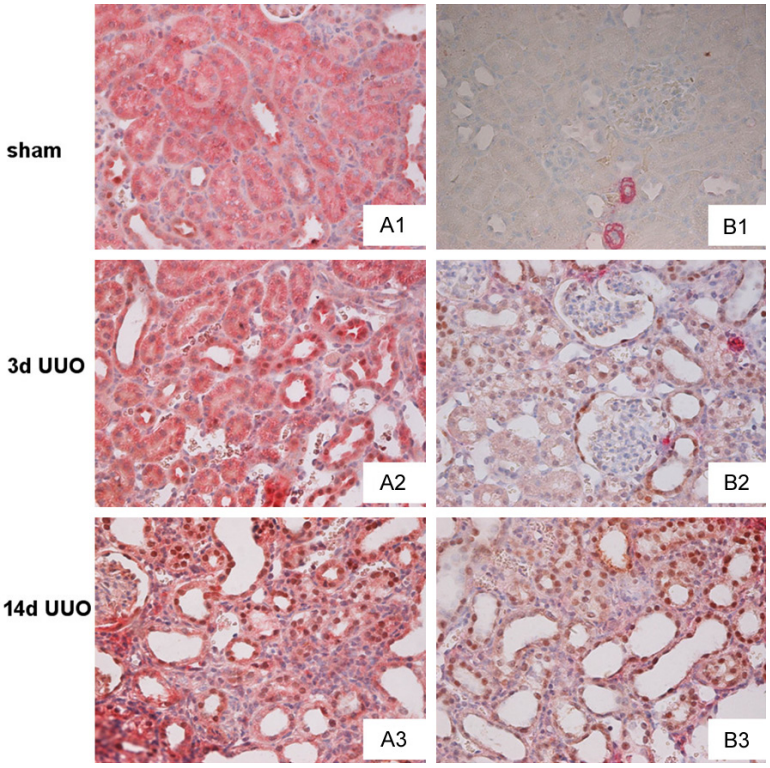

Figure 4. Immunohistochemical double staining for PAX2 and E-cadherin (or α-SMA) was performed. The nuclei of PAX2 immuno-positive cells is stained brown, and membrane- or cytoplasmic-positive staining for E-cadherin or α-SMA, respectively, is stained in red. The co-expression of PAX2/E-cadherin or PAX2/α-SMA is indicated with arrows. Magnification, 200×. PAX2/E-cadherin-positive cells were identified in rats from the sham group (A1), UUO group at day 3 (A2), and UUO group at day 14 (A3). PAX2/α-SMA-positive cells were identified in rats from the sham group (B1), UUO group at day 3 (B2), and UUO group at day 14 (B3).

ed with the sham group (**Figure 3**, P < 0.05). Western blotting also revealed increased levels of α-SMA protein in the obstructed kidneys. In contrast, E-cadherin expression was rapidly downregulated following UUO, ultimately decreasing to undetectable levels by day 14 (P < 0.05).

Co-expression of PAX2/E-cadherin or PAX2/α-SMA and their correlations

In order to determine the relationship between PAX2 and either α-SMA or E-cadherin, double staining of these protein combinations was performed. The nuclei of PAX2 immuno-positive cells were stained brown, and cytoplasmic- or membrane-positive staining for α-SMA or E-cadherin, respectively, was stained in red. In the sham group, the tubular epithelia were completely devoid of PAX2 staining, but showed extensive staining of E-cadherin. Similar to PAX2, expression of α-SMA was also rarely observed, with the exception of some positive staining visible in the small muscular arteries. There was therefore no co-expression between PAX2 and E-cadherin, or PAX2 and α-SMA in control tissue.

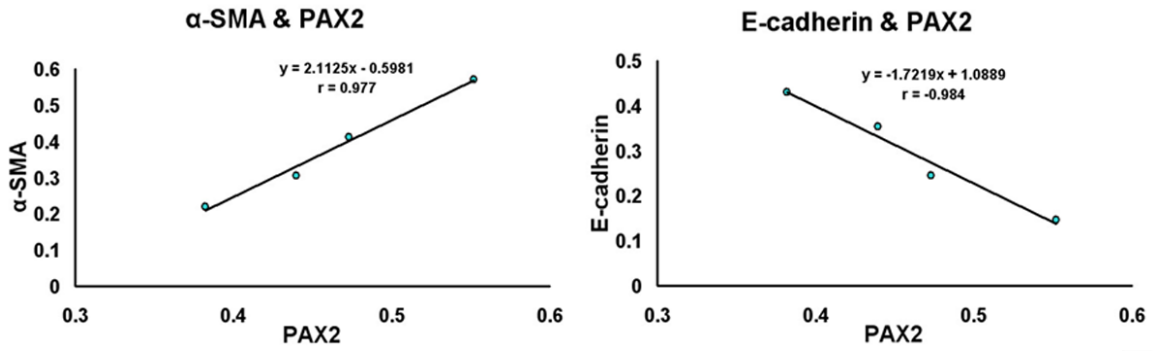

Figure 5. Correlations between data were analyzed using the Pearson test. These analyses revealed that PAX2 protein expression in renal tubules was positively-associated with α-SMA protein levels ($r = 0.977$, $P < 0.05$), and negatively-associated with E-cadherin protein levels ($r = -0.984$, $P < 0.05$).

Three days after the UUO operation, positive staining for PAX2 was detected in the tubular epithelia, while E-cadherin staining was notably decreased. The continuous enhancement of PAX2 expression and simultaneous decrease in E-cadherin expression were observed until day 14. Similar to PAX2, α-SMA expression was significantly enhanced in tubular epithelia and the interstitial area at day 3 following UUO, and its expression consistently increased with prolonged obstruction (**Figure 4**). To determine the significance of this observed correlation, we evaluated the association of PAX2 levels with α-SMA or E-cadherin levels using the Pearson correlation test. These analyses revealed that PAX2 protein expression in renal tubules was positively-associated with α-SMA protein levels ($r = 0.977$, $P < 0.05$), and negatively-associated with E-cadherin protein levels ($r = -0.984$, $P < 0.05$; **Figure 5**).

Discussion

Epithelial cell-cell junctions are important for maintaining both cell polarity and tissue integrity. E-cadherin is encoded by the tumor suppressor gene CDH1, and is a homophilic adhesion molecule that localizes to epithelial adherens junctions [12]. In addition, E-cadherin is known to play a key role in maintaining mature epithelial cells in a differentiated state [13]. It was previously reported that E-cadherin suppresses EMT by down-regulating lymphocyteenhancer factor-1 (LEF-1), which prevents β-catenin nuclear localization. This in turn inhibits Wnt/β-catenin pathway activation that is typically associated with promoting EMT [14, 15]. Therefore, down-regulation of E-cadherin is considered to be one of the key events that driving early EMT initiation. In this study, we revealed that E-cadherin was highly expressed in the renal cortex of control rats. Remarkably, UUO led to a rapid down-regulation in E-cadherin mRNA and protein expression, suggesting that renal epithelial cells ultimately lose their epithelial characteristics following UUO.

RIF is characterized by the accumulation of ECM components and the loss of proper tubular architecture. Excessive production and deposition of interstitial ECM has been attributed to the hyperproliferation of myofibroblasts that results from *de novo* activation of α-SMA. α-SMA is an actin isoform that predominates in vascular and visceral smooth muscle [16]. α-SMA-positive fibroblasts and myofibroblasts have been found in both acute and chronic renal injury [17]. In obstructive nephropathy, activated myofibroblasts stop proliferating and instead produce large amounts of ECM, ultimately resulting in interstitial fibrosis.In this study, α-SMA expression increased rapidly and persistently in obstructed kidneys following UUO, and these changes were consistent with the dramatic ECM accumulation observed. Taken together, the simultaneous decrease in E-cadherin and increase in α-SMA expression observed in these studies further reinforces the conclusion that UUO in renal tissue promotes EMT. The PAX2 genes encode a family of developmentally-controlled proteins that have fundamental roles in kidney development [18]. During embryonic kidney development, PAX2 helps to initiate a genetic cascade, which controls a complex series of events that ultimately

leads to a mesenchymal-to-epithelial conversion [19]. When nephrogenesis is complete, PAX2 is down-regulated and thereafter sustained at very low levels in mature kidneys [20, 21]. In addition, PAX2 was reported to have an anti-apoptotic function, and is likely to be reactivated after renal injury to limit apoptotic damage [22-24]. Following acute tubular necrosis, transient expression of PAX2 was detected in proximal tubular epithelial cells during the process of regeneration [24]. Cohen *et al.* reported that reactivation of PAX2 protects renal collecting duct cells against apoptosis that would typically be induced by obstructive injury [22]. Our previous studies demonstrated that re-expression of PAX2 in a UUO rat model occurs primarily in the renal tubular epithelial cells. Additionally, we showed that PAX2 protein levels positively correlated with both the severity of renal tubular damage and the levels of renal interstitial fibrosis, thus indicating that PAX2 might participate in RIF pathogenesis [25, 26]. To date, however, there has been little evidence of PAX2's direct involvement in renal tubular EMT. In this study, double staining of PAX2/α-SMA and PAX2/E-cadherin was performed to determine whether there was a notable relationship between their expression profiles. In the sham group, tubular epithelia were mostly PAX2- and α-SMA negative, but showed dramatic E-cadherin staining. Interestingly, PAX2 and α-SMA expression gradually increased following UUO and the positively-stained PAX2/α-SMA areas were significantly enhanced by day 14. Contrastingly, E-cadherin expression decreased over the time following obstruction. Pearson correlation analyses further revealed that PAX2 protein levels in renal tubules were positively associated with α-SMA ($r = 0.977$, $P < 0.05$), but not E-cadherin protein levels ($r = -0.984$, $P < 0.05$). These findings suggest that PAX2 re-expression is accompanied by the down-regulation of the epithelial marker E-cadherin and up-regulation of the mesenchymal marker α-SMA. Therefore, PAX2 is likely involved in the process of EMT during renal fibrosis. Furthermore, EMT is generally considered as a reverse process of MET, which occurs during the embryonic development of the mammalian kidney [27]. Given the powerful anti-apoptotic role of PAX2, we hypothesize that PAX2 is re-activated during the early stages of obstructive nephropathy due to a compensatory mechanism. Following obstruction, over-expression of PAX2 not only activates renal tubular epithelial cell transdifferentiation, but also promotes EMT by stimulating complex signaling pathways [9, 28]. Thus, re-expression of PAX2 initially serves as a protective response against renal damage, but ultimately leads to EMT and renal interstitial fibrosis. The molecular mechanism by which PAX2 induces EMT is still unknown and will require further investigation.

Conclusions

In conclusion, the embryonic developmental gene PAX2 is re-expressed in the renal tubular epithelial cells following obstructive nephropathy. PAX2 re-expression is accompanied by up-regulation of the mesenchymal marker α-SMA and down-regulation of the epithelial marker E-cadherin. Therefore, PAX2 likely participates in EMT during the process of renal interstitial fibrosis. Gaining additional insight into PAX2's role in driving EMT would provide ideas for therapeutic approaches to retarding the pathological progression of obstructive nephropathy.

Acknowledgements

Thanks to Professor Yubin Wu at the China Medical University for his assistance with this study. This work was supported by funding from the Youth Science Foundation Projects of Heilongjiang Province (No. QC2012C119), the Key Science and Technology Project of Jiamusi University (No. Sz2014-011), the National Cultivating Project of Jiamusi University (No. JMSUJCGP2016-005) and the Youth academic backbone support project of Heilongjiang Province (No. 1253G057).

Disclosure of conflict of interest

None.

Address correspondence to: Chang-Shan Wang, College of Basic Medicine, Jiamusi University, No. 148 Xuefu St, Jiamusi 154007, Heilongjiang, China. Tel: +88613945470064; Fax: +88613945470064; E-mail: wcs0451@163.com

References

[1] Kushiyama T, Oda T, Yamada M, Higashi K, Yamamoto K, Sakurai Y, Miura S and Kumagai H. Alteration in the phenotype of macrophages in the repair of renal interstitial fibrosis in mice. Nephrology (Carlton) 2011; 16: 522-535.

[2] Xie XS, Liu HC, Wang FP, Zhang CL, Zuo C, Deng Y and Fan JM. Ginsenoside Rg1 modulation on thrombospondin-1 and vascular endothelial growth factor expression in early renal fibrogenesis in unilateral obstruction. Phytother Res 2010; 24: 1581-1587.
[3] Bascands JL and Schanstra JP. Obstructive nephropathy: insights from genetically engineered animals. Kidney Int 2005; 68: 925-937.
[4] Razzaque MS and Taguchi T. Cellular and molecular events leading to renal tubulointerstitial fibrosis. Med Electron Microsc 2002; 35: 68-80.
[5] Chevalier RL. Chronic partial ureteral obstruction and the developing kidney. Pediatr Radiol 2008; 38 Suppl 1: S35-40.
[6] Liu Y. Epithelial to mesenchymal transition in renal fibrogenesis: pathologic significance, molecular mechanism, and therapeutic intervention. J Am Soc Nephrol 2004; 15: 1-12.
[7] Wynn TA. Cellular and molecular mechanisms of fibrosis. J Pathol 2008; 214: 199-210.
[8] Kalluri R and Weinberg RA. The basics of epithelial-mesenchymal transition. J Clin Invest 2009; 119: 1420-1428.
[9] Li L, Wu Y and Yang Y. Paired box 2 induces epithelial-mesenchymal transition in normal renal tubular epithelial cells of rats. Mol Med Rep 2013; 7: 1549-1554.
[10] Zhou TB. Signaling pathways of PAX2 and its role in renal interstitial fibrosis and glomerulosclerosis. J Recept Signal Transduct Res 2012; 32: 298-303.
[11] Murer L, Caridi G, Della Vella M, Montini G, Carasi C, Ghiggeri G and Zacchello G. Expression of nuclear transcription factor PAX2 in renal biopsies of juvenile nephronophthisis. Nephron 2002; 91: 588-593.
[12] Taso CJ, Lin HS, Lin WL, Chen SM, Huang WT and Chen SW. The effect of yoga exercise on improving depression, anxiety, and fatigue in women with breast cancer: a randomized controlled trial. J Nurs Res 2014; 22: 155-164.
[13] Sun S, Sun W, Xia L, Liu L, Du R, He L, Li R, Wang H and Huang C. The T-box transcription factor brachyury promotes renal interstitial fibrosis by repressing E-cadherin expression. Cell Commun Signal 2014; 12: 76.
[14] Orsulic S, Huber O, Aberle H, Arnold S and Kemler R. E-cadherin binding prevents beta-catenin nuclear localization and beta-catenin/LEF-1-mediated transactivation. J Cell Sci 1999; 112: 1237-1245.
[15] Zhao JH, Luo Y, Jiang YG, He DL and Wu CT. Knockdown of beta-catenin through shRNA cause a reversal of EMT and metastatic phenotypes induced by HIF-1alpha. Cancer Invest 2011; 29: 377-382.
[16] Arnoldi R, Hiltbrunner A, Dugina V, Tille JC and Chaponnier C. Smooth muscle actin isoforms: a tug of war between contraction and compliance. Eur J Cell Biol 2013; 92: 187-200.
[17] Strutz F and Zeisberg M. Renal fibroblasts and myofibroblasts in chronic kidney disease. J Am Soc Nephrol 2006; 17: 2992-2998.
[18] Narlis M, Grote D, Gaitan Y, Boualia SK and Bouchard M. Pax2 and pax8 regulate branching morphogenesis and nephron differentiation in the developing kidney. J Am Soc Nephrol 2007; 18: 1121-1129.
[19] Rothenpieler UW and Dressler GR. Pax-2 is required for mesenchyme-to-epithelium conversion during kidney development. Development 1993; 119: 711-720.
[20] Luu VD, Boysen G, Struckmann K, Casagrande S, von Teichman A, Wild PJ, Sulser T, Schraml P and Moch H. Loss of VHL and hypoxia provokes PAX2 up-regulation in clear cell renal cell carcinoma. Clin Cancer Res 2009; 15: 3297-3304.
[21] Zhou TB, Qin YH, Zhou C, Lei FY, Zhao YJ, Chen J, Su LN and Huang WF. Less expression of prohibitin is associated with increased caspase-3 expression and cell apoptosis in renal interstitial fibrosis rats. Nephrology (Carlton) 2012; 17: 189-196.
[22] Cohen T, Loutochin O, Amin M, Capolicchio JP, Goodyer P and Jednak R. PAX2 is reactivated in urinary tract obstruction and partially protects collecting duct cells from programmed cell death. Am J Physiol Renal Physiol 2007; 292: F1267-1273.
[23] Dziarmaga A, Hueber PA, Iglesias D, Hache N, Jeffs A, Gendron N, Mackenzie A, Eccles M and Goodyer P. Neuronal apoptosis inhibitory protein is expressed in developing kidney and is regulated by PAX2. Am J Physiol Renal Physiol 2006; 291: F913-920.
[24] Imgrund M, Grone E, Grone HJ, Kretzler M, Holzman L, Schlondorff D and Rothenpieler UW. Re-expression of the developmental gene Pax-2 during experimental acute tubular necrosis in mice 1. Kidney Int 1999; 56: 1423-1431.
[25] Li L, Wu Y, Wang C and Zhang W. Inhibition of PAX2 gene expression by siRNA (polyethylenimine) in experimental model of obstructive nephropathy. Ren Fail 2012; 34: 1288-1296.
[26] Li L, Wu Y and Zhang W. PAX2 re-expression in renal tubular epithelial cells and correlation with renal interstitial fibrosis of rats with obstructive nephropathy. Ren Fail 2010; 32: 603-611.
[27] Horster MF, Braun GS and Huber SM. Embryonic renal epithelia: induction, nephrogenesis, and cell differentiation. Physiol Rev 1999; 79: 1157-1191.
[28] Lindoso RS, Verdoorn KS and Einicker-Lamas M. Renal recovery after injury: the role of Pax-2. Nephrol Dial Transplant 2009; 24: 2628-2633.